Interaction mechanism for energy transfer from Ce to Tb ions in silica

HAA Seed Ahmed[1,2], W-S Chae[3], OM Ntwaeaborwa[1] and RE Kroon[1]

[1]Department of Physics, University of the Free State, South Africa
[2]Department of Physics, University of Khartoum, Sudan
[3]Korea Basic Science Institute (KBSI), Gangneung, Korea

E-mail: KroonRE@ufs.ac.za

Abstract: Energy transfer phenomena can play an important role in the development of luminescence materials. In this study, numerical simulations based on theoretical models of non-radiative energy transfer are compared to experimental results from Ce,Tb co-doped silica. Energy transfer from the donor (Ce) to the acceptor (Tb) resulted in a decrease in the Ce luminescence intensity and lifetime. The decrease in intensity corresponded well with the energy transfer models based on the exchange interaction and the dipole-dipole interaction. The critical transfer distance obtained from the fitting using both models is around 20 Å. Since the exchange interaction requires a distance shorter than 10 Å to occur, the mechanism for energy transfer was identified as the dipole-dipole interaction. This conclusion is supported by an analysis of the lifetime data.

1. Introduction

Energy transfer phenomena can play an important role in the development of luminescence materials. For example, the green luminescence from Tb^{3+} doped silica can be excited efficiently using a very short wavelength UV light near 227 nm [1]. However, the excitation wavelength can be shifted to a more accessible value of 325 nm by co-doping Tb^{3+} with Ce^{3+} ions. At this wavelength Ce^{3+} ions absorb and then transfer the energy to the Tb^{3+} ions. Many theoretical and experimental studies have been done on non-radiative energy transfer since Forster first treated it theoretically [2-7]. The process involves excitation of a donor followed by transfer of the excitation energy to an acceptor. Non-radiative energy transfer can be distinguished from radiative energy transfer, for which the acceptor absorbs the radiation (photon) emitted by the donor, by the fact that in the first case energy transfer is associated with a decrease in the donor lifetime, while in the second case the donor lifetime is not affected.

Forster developed a theory for the rate of non-radiative energy transfer by electric dipole-dipole interaction [2]. This was later extended by Dexter to involve the higher multipole interactions [3]. Dexter also created a model for shorter donor-acceptor distances based on the exchange interaction [3]. The transfer mechanisms differ according to the dependence of the transfer rate on the donor-acceptor distance. Inokuti and Hirayama [8] developed numerical methods on energy transfer that determine the mechanism responsible. Nakazawa and Shionoya [9] used these calculations to study the energy transfer between unlike trivalent rare-earth ions in glass. They found that the dipole-quadrupole interaction gave

the best fit between theory and experiment. Mares *et al.* [10] investigated the mechanism of the energy transfer between Ce and Nd in YAG:Nd,Ce by fitting the decay curves of Ce to the theory of Inokuti and Hirayama [8] and reported that both dipole-dipole and dipole-quadrupole mechanisms contribute to energy transfer. In this study, the theoretical calculations of Inokuti and Hirayama [8] are implemented in MATLAB and compared to experimental data to investigate the mechanism of the energy transfer from Ce to Tb in sol-gel silica.

2. Experimental
A series of 14 Ce,Tb co-doped silica samples with a fixed concentration of Ce (0.5 mol%) and varying concentration of Tb from 0 up to 0.8 mol% were produced by the sol-gel method. Tetraethylorthosilicate (TEOS), water, $Ce(NO_3)_3.6H_2O$, and $Tb(NO_3)_3.6H_2O$ were used as starting materials, ethanol (C_2H_5OH) as a solvent and nitric acid (HNO_3) as a catalyst. An amount of 11.15 ml of TEOS (0.05 M) was mixed with 10 ml of ethanol and stirred for 30 minutes, after which 9 ml of water (containing 0.15 M HNO_3) was added. Stirring then continued for another 30 minutes, after which the appropriate amount of dissolved $Ce(NO_3)_3.6H_2O$ and $Tb(NO_3)_3.6H_2O$ in ethanol was added to the mixture, which was stirred for a further 4 h. The mixture was then stored in a closed container and transferred to a water bath at 50°C until a gel was formed. The gel was dried, crushed and annealed at 1000°C in flowing 4% hydrogen in argon gas for 2 hours. To control the concentration of the dopants accurately, an appropriate amount of $Ce(NO_3)_3.6H_2O$ was dissolved in 75 ml of ethanol so that each 5 ml contained the required concentration (0.5 mol%) of Ce ions. An appropriate amount of $Tb(NO_3)_3.6H_2O$ was also dissolved in 10 ml of ethanol. Of this mixture, 5 ml was added to produce the highest concentration of Tb ions. The remainder was diluted to 10 ml by adding ethanol, of which half was used to produce the next concentration of Tb ions (half of the first one). This process was repeated until the lowest concentration of Tb ions was reached.

Photoluminescence (PL) measurements were made at room temperature using a Cary Eclipse fluorescence spectrophotometer equipped with a xenon lamp. Fluorescence lifetime measurements were performed on a time-resolved fluorescence confocal microscope (MicroTime-200, PicoQuant, Germany). A single-mode pulsed diode laser (375 nm) with a pulse width of ~240 ps in full-width at half maximum and an average power less than 1 μW was used as an excitation source. Data acquisition was based on a time-correlated single-photon counting (TCSPC) technique.

3. Theoretical considerations
The non-radiative transfer of an electronic excitation from a donor to an acceptor can be represented by
$$D^* + A \rightarrow D + A^* \tag{1}$$
where D represents the ground state of the donor and A the ground state of the acceptor, and D^* and A^* represent their excited states. It has been shown that the transfer rate between the initial and final states is given by [11]
$$W_{DA} = \frac{2\pi}{\hbar} |\langle DA^*|\mathcal{H}_{DA}|D^*A\rangle|^2 \int f_D(E)f_A(E)dE \tag{2}$$
where $\langle DA^*|$ is the final state, $|D^*A\rangle$ is the initial state and $\mathcal{H}_{DA}$ is the interaction Hamiltonian. The integral represent the spectral overlap between the donor (D) emission spectrum and the acceptor (A) absorption spectrum. The normalised emission spectrum of the donor is $f_D(E)$ and the normalised absorption spectrum of the acceptor is $f_A(E)$. The mechanism for energy transfer depends on the interaction Hamiltonian.

If the wavefunctions of the donor and acceptor overlap, the quantum mechanical exchange interaction results in a transfer rate [4]
$$W_{DA} = \frac{1}{\tau_0} \exp\left(\frac{2R_0}{L}\left[1-\frac{r}{R_0}\right]\right) \tag{3}$$

where τ_0 is the donor lifetime in the absence of the acceptor, r is the distance between donor and acceptor, R_0 is the so-called critical separation distance for which energy is transferred at the same rate as which it decreases via luminescence when no acceptors are present, and L is a scaling factor corresponding to an effective Bohr radius. The corresponding decay function $\phi(t)$ after pulse excitation is given by [8]

$$\phi(t) = \exp\left[\frac{-t}{\tau_0} - \gamma^{-3}\frac{c}{c_0}g(\frac{t}{\tau_0}e^\gamma)\right] \qquad (4)$$

where the exchange constant γ is related to the scaling factor L by $\gamma = 2R_0/L$ and $g\left(\frac{t}{\tau_0}e^\gamma\right)$ is a function that can be evaluated numerically [8], while c is the acceptor concentration and c_0 is the critical concentration related to the critical radius by

$$c_0 = 3/(4\pi R_0^3). \qquad (5)$$

For larger separation distances non-radiative energy transfer may occur via electric multipole interactions, resulting in an energy transfer rate [3]

$$W_{DA} = \frac{1}{\tau_0}\left(\frac{R_0}{r}\right)^s \qquad (6)$$

where s = 6 for dipole-dipole, 8 for dipole-quadrupole and 10 for quadrupole-quadrupole interactions. The corresponding decay function is [8]

$$\phi(t) = \exp\left[\frac{-t}{\tau_0} - \Gamma\left(1 - \frac{3}{s}\right)\frac{c}{c_0}\left(\frac{t}{\tau_0}\right)^{3/s}\right]. \qquad (7)$$

As a result of energy transfer, the luminescence intensity as well as the lifetime of the donor decreases. Inokuti and Hirayama [8] developed numerical methods to simulate these changes for the different interactions mechanisms. The relative emission intensity of the donor can be calculated from

$$\frac{I}{I_0} = \frac{1}{\tau_0}\int_0^\infty \phi(t)dt \qquad (5)$$

where I is the donor emission intensity in the presence of the acceptor, and I_0 the corresponding intensity in the absence of acceptors. Similarly, the mean decay time τ_m can be calculated from

$$\tau_m = \int_0^\infty t\phi(t)dt / \int_0^\infty \phi(t)dt. \qquad (6)$$

MATLAB was used to calculate the theoretical decay functions $\phi(t)$ as well as the relative emission intensities $\frac{I}{I_0}$ and the reduced mean decay times $\frac{\tau_m}{\tau_0}$ as a function of the concentration c/c_0 for the different energy transfer mechanisms in order to compare these theoretical results to experimental data.

4. Results and discussion

For luminescence measurements all the samples were excited at the Ce absorption band near 325 nm [12]. The Ce luminescence with a short lifetime (in the ns order) was recorded with the Cary Eclipse spectrometer in fluorescence mode, while the Tb luminescence with a long lifetime (in the ms order) was recorded in the phosphorescence mode. Figure 1 presents the PL emission of Ce and Tb for the samples having Tb concentrations of 0.0100 and 0.800 mol%. The reduction of the Ce emission and increase of the Tb emission while exciting the Ce shows that energy transfer occurs. Table 1 (columns 2 and 3) lists the emission intensity (I) and the relative emission intensity ($\frac{I}{I_0}$) of the Ce donor for all the samples.

The experimental values of $\frac{I}{I_0}$ were fitted to the theoretical curve using the least squares method in MATLAB. For the multipole interaction mechanisms (dipole-dipole, dipole-quadrupole and quadrupole-quadrupole) the fitting parameter is the critical concentration c_0, while for the exchange interaction mechanism the exchange constant γ is fitted in addition to c_0, . The results are shown Figure 2 and the fit parameters are listed in Table 2. The standard deviation (σ) of the experimental data from its theoretical curve was also calculated for each interaction. The best fit was obtained for the exchange model, but it should be noted that for this fit there are two fitting parameters. The best fit amongst the multipole interaction models was for the dipole-dipole interaction. For all the models the critical distance R_0 was

around 20 Å. The exchange interaction requires an overlap of wavefunctions and is only realistic for very small critical distances ($R_0 \leq 10$ Å) [13]. Therefore, although the fit is good, the energy transfer cannot be attributed to the exchange interaction and the dipole-dipole interaction seems most probable mechanism.
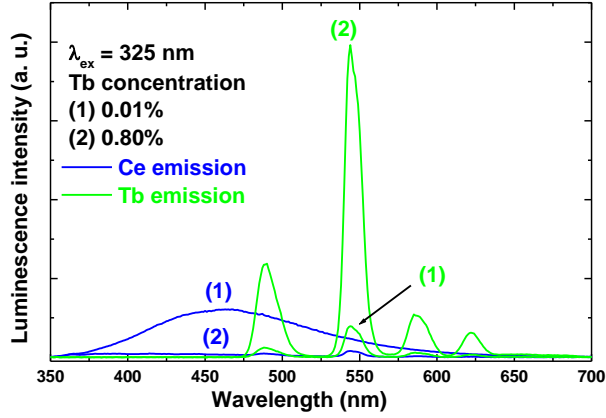

Figure 1. PL emission of (1) SiO$_3$:Ce(0.5%),Tb(0.01%) and (2) SiO$_3$:Ce (0.5%),Tb(0.80%). The Ce emission was recorded in fluorescence mode while the Tb emission was recorded in phosphorescence mode from the same samples.

Table 1. Acceptor concentration, Donor emission intensity and lifetime of the all series.

Acceptor concentration (mol%)	Donor emission intensity		Donor lifetime	
	I (a.u.)	$\dfrac{I}{I_0}$	τ_m (ns)	$\dfrac{\tau_m}{\tau_0}$
0	64.6	1	50	1
0.0100	60.2	0.932	42	0.84
0.0160	54.6	0.845	41	0.82
0.0200	52.9	0.819	42	0.84
0.0310	44.8	0.693	39	0.78
0.0400	39.7	0.615	38	0.76
0.0630	31.1	0.481	31	0.62
0.0800	22.4	0.347	22	0.44
0.125	17.3	0.268	25	0.50
0.200	11.0	0.170	17	0.34
0.250	9.18	0.142	15	0.30
0.400	6.00	0.093	16	0.32
0.500	5.84	0.090	10	0.20
0.800	3.38	0.052	8.0	0.16

Table 2 Parameters obtained from the fitted data

Type of interaction	γ or s	c_0 (mol%)	R_0 (Å)	$\sigma (\times 10^{-2})$
Exchange	4	0.12	19. 6	2.9
Dipole-dipole	6	0.12	19.6	3.3
Dipole-quadrupole	8	0.11	20.8	3.7
Quadrupole-quadrupole	10	0.10	21.5	4.0

Lifetime decay curves of the Ce donor emission are presented in Figure 3 after excitation with a pulsed laser at 375 nm. The f-d excitation peak for Ce in silica is at 325 nm (which was used for the PL measurements), but it is very broad and extends to the wavelength used for the lifetime measurements. The Ce emission was monitored using a bandpass filter (450 ± 20 nm). Although blue emission from the $^5D_3$ levels of Tb can occur in this region, blue emission from the Tb after energy transfer from the Ce was not observed in the samples, even for the low Tb concentrations when cross-relaxation would not occur [13]. It is suggested that this is because the energy transfer from the Ce to Tb excites the $^5D_4$ level rather than the higher $^5D_3$ level.
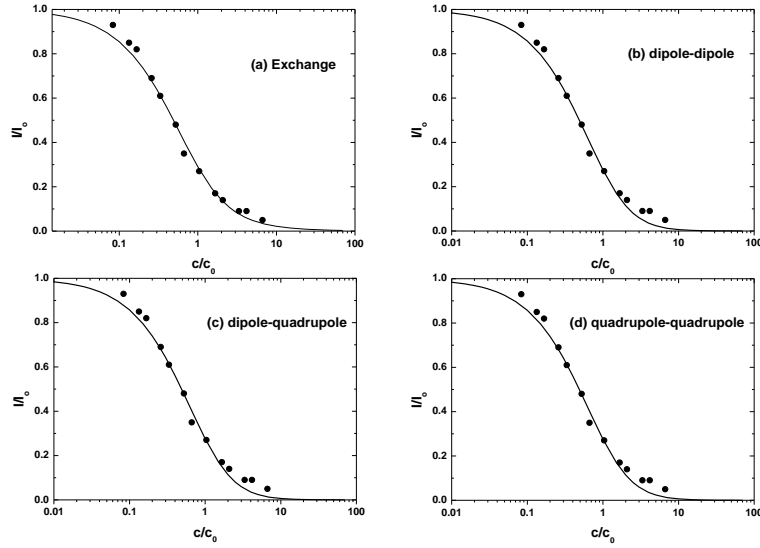
Figure 2 Experimental data of the relative emission intensity of the donor $\frac{I}{I_0}$ (open circles) vs acceptor concentration $\frac{c}{c_0}$ fitted to the theoretical curve (solid) for the case of (a) exchange, (b) dipole-dipole, (c) dipole-quadrupole, and (d) quadrupole-quadrupole interaction models.
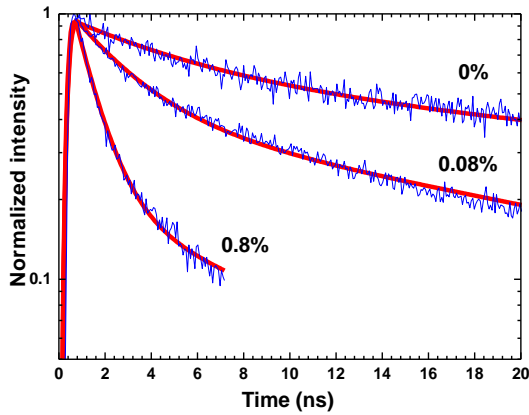

Figure 3. The decay curve of the samples SiO_3:Ce (x%) where x is 0%, 0.08% and 0.8%. The blue curve is the measured data and the red points are the convolution of the fitted data.

Although the decay curve of the Ce singly doped sample (Figure 3) is not simple exponential, a dramatic shortening of the lifetime was measured for samples co-doped with Tb, as expected for non-radiative energy transfer. Possible reasons for the deviation from simple exponential decay for the Ce singly doped sample are that the Ce occupies more than one site in the amorphous host, or that there is some contribution to the emission from defects in the silica. The measured decay data for a period until the curve had decayed to 10% of its maximum value was fit to a multiexponential function (two exponentials were found to be adequate) that had been convoluted with the instrument response function, using least squares fitting in MATLAB. The fitted multiexponential functions were then used to compute the mean lifetimes, which are given in Table 1 (column 4). The mean lifetime of the Ce singly doped sample was 50 ns and this value was used for τ_0. The experimental values of $\frac{\tau_m}{\tau_0}$ were fit to the theoretical curve for the dipole-dipole interaction mechanism and the result in shown in Figure 4. Although the experimental decay data shows some scatter, the critical concentration for the fit was 0.12 mol% which corresponds exactly to what was found from the relative intensity data (Table 2). Figure 5 shows the plot of the experimental values of $\frac{I}{I_0}$ versus $\frac{\tau_m}{\tau_0}$ compared to the theoretical curves for the different types of multipole interaction, and from this data one can also see that the dipole-dipole interaction mechanism is the most probably mechanism for energy transfer between Ce and Tb in silica.
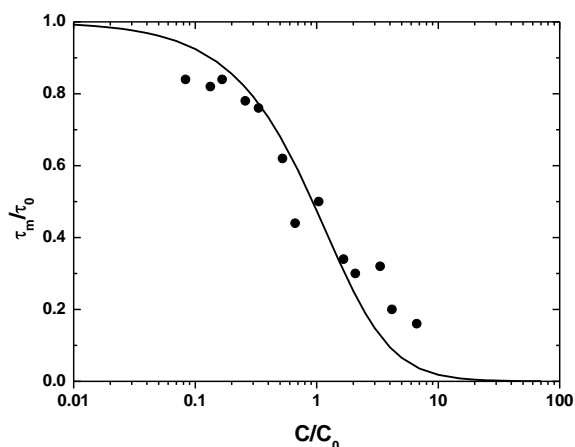
Figure 4 Experimental data of the decay lifetime $\frac{\tau_m}{\tau_0}$ of the donor (dotted circles) vs acceptor concentration $\frac{c}{c_0}$ fitted to the dipole-dipole theoretical curve (solid).
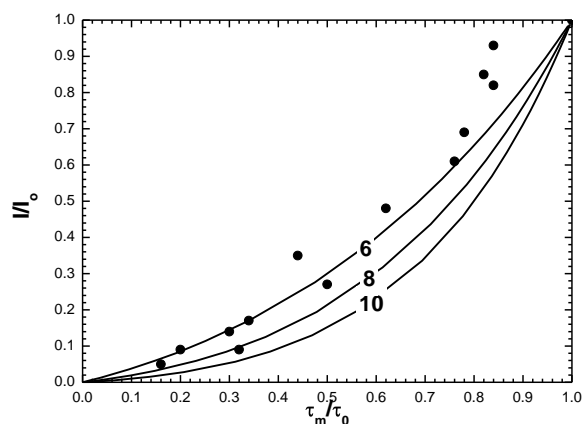
Figure 5 The relative emission intensity $\frac{I}{I_0}$ vs the decay lifetime $\frac{\tau_m}{\tau_0}$ of the donor (dotted circles) fitted to the theoretical curves (solid) for the multipole interaction

5. Conclusion

The mechanism of the energy transfer from Ce to Tb in sol-gel silica was investigated using the Inokuti and Hirayama models. The relative emission intensity of the donor ($\frac{I}{I_0}$) as a function of the acceptor concentration was found to fit well to the theoretical curves associated with the exchange interaction model and the dipole-dipole interaction model, with the critical distance R_0 around 20 Å for both models. The obtained value of R_0 leads us to exclude the exchange interaction model, which requires shorter distances ($R_0 \leq 10$ Å). The mechanism for energy transfer is therefore suggested to be due to dipole-dipole interactions. This conclusion is supported by an analysis of the lifetime data.

References

[1]   Kroon RE, Seed Ahmed HAA and Gusowski MA 2011 *Proceedings of SAIP2011*, the 56th Annual Conference of the South African Institute of Physics, edited by I. Basson and A.E. Botha (University of South Africa, Pretoria, 2011), p. 162. ISBN: 978-1-86888-688-3. Available online at http:\\www.saip.org.za.
[2]   Forster Th 1948 *Ann. Physik* **2** 55
[3]   Dexter DL 1953 *J. Chem. Phys.* **21** 836
[4]   Walter JCG 1971 *Phys. Rev.* B **4** 648
[5]   Lenth W and Huber G 1981 *Phys. Rev.* B **23** 3877
[6]   Bojarski C, Grabowska J, Kulak L and Kusba J 1991 *J. Fluoresc.* **1** 183
[7]   Morita M, Buddhudu S, Rau D and Murakami S 2004 *Struct. Bonding* **107** 115
[8]   Inokuti M and Hirayama F 1965 *J. Chem. Phys.* **43** 1978
[9]   Nakazawa E and Shionoya S 1967 *J. Chem. Phys.* **47** 3211
[10]   Mares J, Jacquier B, Pedrini C and Boulon G 1987 *Revue Phys. Appl.* **22** 145
[11]   Vasquez SO 1999 *Physical Rev. B* **60** 8575
[12]   Xu GQ Zheng ZX Tang WM and Wu YC 2007 *J. Lumin.* **124** 151
[13]   Blasse G 1983 *Rev. Inorg. Chem.* **15** 319